

Pseudomagnetic helicons

E. V. Gorbar,^{1,2} V. A. Miransky,^{3,4} I. A. Shovkovy,^{5,6} and P. O. Sukhachov³

¹*Department of Physics, Taras Shevchenko National Kiev University, Kiev, 03680, Ukraine*

²*Bogolyubov Institute for Theoretical Physics, Kiev, 03680, Ukraine*

³*Department of Applied Mathematics, Western University, London, Ontario N6A 5B7, Canada*

⁴*Department of Physics and Astronomy, Western University, London, Ontario N6A 3K7, Canada*

⁵*College of Integrative Sciences and Arts, Arizona State University, Mesa, Arizona 85212, USA*

⁶*Department of Physics, Arizona State University, Tempe, Arizona 85287, USA*

(Dated: December 21, 2016)

The existence of pseudomagnetic helicons is predicted for strained Weyl materials. The corresponding collective modes are similar to the usual helicons in metals in strong magnetic fields but can exist even without a magnetic field due to a strain-induced background pseudomagnetic field. The properties of both pseudomagnetic as well as magnetic helicons are investigated in Weyl matter using the formalism of the consistent chiral kinetic theory. It is argued that the helicon dispersion relations are affected by the electric and chiral chemical potentials, the chiral shift, and the energy separation between the Weyl nodes. The equilibrium as well as non-equilibrium regimes of Weyl matter are discussed. A simple setup for experimental detection of pseudomagnetic helicons is proposed.

PACS numbers: 71.45.-d, 03.65.Sq

Keywords: Weyl materials, chiral kinetic theory, collective excitations, helicons, pseudomagnetic field

I. INTRODUCTION

Electromagnetic collective excitations play an important role in various plasmas [1–4] including relativistic ones. The latter are usually studied in the context of the early Universe [5, 6], the relativistic heavy-ion collisions [7, 8], and degenerate states of dense matter in compact stars [9]. Since the low-energy quasiparticle excitations in the recently discovered Dirac [10–12] and Weyl [13–18] materials are described by the massless Dirac/Weyl equations, the properties of their collective effects should resemble those in relativistic plasmas. By taking into account that the massless Dirac/Weyl quasiparticles carry a well defined chirality, an imbalance between the number densities of opposite chirality carriers could be induced. Such a chiral asymmetry opens the possibility of qualitatively new effects and could modify the properties of collective excitations in the relativistic-like quasiparticle plasma.

It is worth pointing out that the Dirac and Weyl materials may not only reveal some characteristic properties of truly relativistic forms of matter but also allow one to probe absolutely new quantum effects inaccessible in high-energy physics. Some of them, for example, are connected with the unusual plasma response to a background pseudomagnetic field \mathbf{B}_5 . Unlike an ordinary magnetic field \mathbf{B} , a pseudomagnetic field \mathbf{B}_5 couples with different signs to fermions of different chiralities. In Weyl and Dirac materials, the pseudomagnetic field can be induced by various types of strains [19–23]. In the case of Cd_3As_2 material, for example, it is estimated that the magnitude of the corresponding field could reach about $B_5 \approx 0.3$ T when a static torsion is applied to a nanowire [23] and about $B_5 \approx 15$ T when a thin film is bent [24]. Since Weyl nodes in condensed matter materials always come in pairs of opposite chirality (this stems from the Nielsen–Ninomiya theorem [25]), the pseudomagnetic field by itself does not break the time reversal symmetry in Weyl materials.

Plasmons are perhaps the best known and characteristic collective excitations in plasma. They are gapped excitations whose minimal energy is determined by the plasma frequency. Recently, we showed [26, 27] that plasmons in relativistic matter in constant magnetic and pseudomagnetic fields are, in fact, *chiral* (pseudo-)magnetic plasmons whose chiral nature is manifested in the oscillations of the chiral charge density, which are absent for ordinary electromagnetic plasmons. Moreover, the constant pseudomagnetic field \mathbf{B}_5 affects the dependence of plasmon frequencies already in the linear order in the wave-vector. Similar modifications to the energy dispersion of these plasmons can be also induced by the chiral shift parameter \mathbf{b} (i.e., the momentum-space separation of the Weyl nodes) in Weyl materials. Interestingly, even in the absence of the chiral shift and external fields, the chiral chemical potential leads to a splitting of the plasmon frequencies in the linear order in the wave vector [27].

For a long time it was believed that low frequency electromagnetic waves cannot propagate in metals. However, the authors of Refs. [28, 29] showed that there exist transverse low-energy gapless excitations propagating along the background magnetic field in uncompensated metals (i.e., metals with different electron and hole densities), which were called helicons. Their counterparts propagating in ionospheres of planets are known as whistlers. Pioneer study of helicons in Weyl materials was performed in Ref. [30], where it was shown that the dispersion law of these collective excitations encodes information on the chiral shift parameter \mathbf{b} . In this paper, we extend the corresponding study

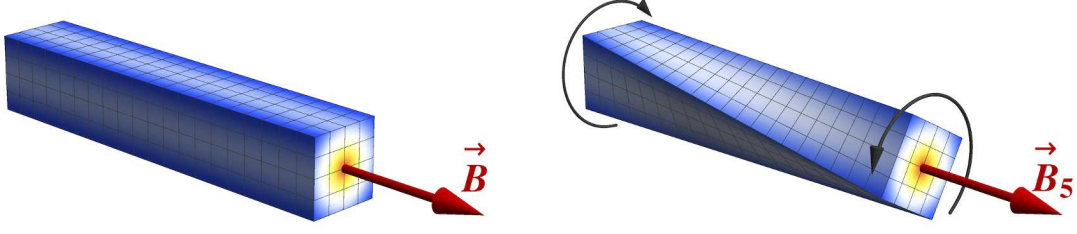


FIG. 1. The illustration of two limiting setups for observing helicons. While the usual helicons can be induced in Weyl materials in a background magnetic field (left panel), the pseudomagnetic helicons should exist in Weyl materials with torsion/strain induced pseudomagnetic field (right panel).

to the case of a background pseudomagnetic field, a nonzero chiral chemical potential, and temperature. The two limiting setups for observing helicons with magnetic \mathbf{B} and pseudomagnetic \mathbf{B}_5 fields are schematically illustrated in the left and right panels in Fig. 1, respectively. Using the consistent chiral kinetic theory, we show that a new type of collective excitations, namely, a *pseudomagnetic helicon* exists in Weyl materials under strain.

The paper is organized as follows. The polarization vector and the characteristic equation for the low-energy collective excitations are derived in Sec. II. The pseudomagnetic helicons are analyzed in Sec. III. The main results are summarized in Sec. IV. In Appendix A, we present the key details of the consistent chiral kinetic theory. Some useful technical formulas and results are given in Appendices B and C.

II. POLARIZATION VECTOR AND CHARACTERISTIC EQUATION

In this section, we use the consistent chiral kinetic theory [26, 27] in order to derive the polarization vector and the characteristic equation for the low-energy collective excitations in Weyl materials in an effective background field $\mathbf{B}_{0,\lambda} \equiv \mathbf{B}_0 + \lambda \mathbf{B}_{0,5}$, where \mathbf{B}_0 is an ordinary magnetic field, $\mathbf{B}_{0,5}$ is a strain-induced pseudomagnetic field, and $\lambda = \pm$ is the fermion chirality. It should be noted that the consistent formulation of the kinetic theory amends the original formulation of Refs. [31–33] to the case of Weyl materials with a nonzero chiral shift parameter \mathbf{b} (odd under time reversal symmetry) and the energy separation between the Weyl nodes b_0 (odd under the parity transformation). Moreover, in the presence of pseudo-electromagnetic fields, the consistent formulation of the chiral kinetic theory [26, 27] is required by the local conservation of the electric charge. (For similar arguments in the context of quantum field theory, see Refs. [34, 35].) Such a formulation is also essential for the correct description of the anomalous Hall effect in Weyl materials [36, 37], as well as for ensuring the absence of the chiral magnetic effect (CME) current in an equilibrium state of Weyl matter [35, 38, 39].

In this study we assume that a Weyl material is subjected only to static background magnetic fields and strains. Therefore, pseudoelectric as well as background electric fields are absent, $\mathbf{E}_0 = \mathbf{E}_{0,5} = 0$. Furthermore, for simplicity, we set $\mathbf{B}_0 \parallel \hat{\mathbf{z}}$ and $\mathbf{B}_{0,5} \parallel \hat{\mathbf{z}}$, where $\hat{\mathbf{z}}$ denotes the unit vector pointing in the $+z$ -direction. In addition to the background magnetic and pseudomagnetic fields, collective modes in Weyl materials may induce weak oscillating electromagnetic fields \mathbf{E}' and \mathbf{B}' . As usual in the linear regime [1, 2], the corresponding fields take the form of plane waves, i.e.,

$$\mathbf{E}' = \mathbf{E} e^{-i\omega t + i\mathbf{k} \cdot \mathbf{r}}, \quad \mathbf{B}' = \mathbf{B} e^{-i\omega t + i\mathbf{k} \cdot \mathbf{r}}, \quad (1)$$

with frequency ω and wave vector \mathbf{k} . The Maxwell equations imply that $\mathbf{B}' = c(\mathbf{k} \times \mathbf{E}')/\omega$ and

$$\mathbf{k}(\mathbf{k} \cdot \mathbf{E}') - k^2 \mathbf{E}' = -\frac{\omega^2}{c^2} (n_0^2 \mathbf{E}' + 4\pi \mathbf{P}'), \quad (2)$$

where

$$P'^m \equiv P^m e^{-i\omega t + i\mathbf{k} \cdot \mathbf{r}} = i \frac{J'^m}{\omega} = \chi^{ml} E'^l \quad (3)$$

is the polarization vector, J'^m is the oscillating part of the current, see Eq. (A10), χ^{ml} is the electric susceptibility tensor, and $m, l = 1, 2, 3$ denote spatial indices. Further, n_0 denotes the material's refractive index, which in the case of Dirac semimetal Cd_3As_2 is $n_0 \approx 6$ [40]. In order to simplify our analysis here, we will neglect the dependence of

the refractive index on the frequency. This is well justified for a relatively narrow range of frequencies relevant for helicon modes. From Eq. (2) we derive the following characteristic equation:

$$\det \left[(n_0^2 \omega^2 - c^2 k^2) \delta^{lm} + c^2 k^l k^m + 4\pi \omega^2 \chi^{lm} \right] = 0. \quad (4)$$

The electric susceptibility tensor χ^{lm} can be determined by using the consistent chiral kinetic theory. The key details of the corresponding formalism are reviewed in Appendix A. In the study of collective excitations, it is convenient to use the following ansatz for the distribution function $f_\lambda = f_\lambda^{(\text{eq})} + \delta f_\lambda$, where $f_\lambda^{(\text{eq})}$ is the equilibrium distribution function given in Eq. (A5), and

$$\delta f_\lambda = f_\lambda^{(1)} e^{-i\omega t + i\mathbf{k} \cdot \mathbf{r}} \quad (5)$$

is a perturbation related to the oscillating fields \mathbf{E}' and \mathbf{B}' . To the leading order in perturbation theory, the chiral kinetic equation (A1) takes the form

$$i \left[(1 + \kappa_\lambda) \omega - (\mathbf{v} \cdot \mathbf{k}) - \frac{e}{c} (\mathbf{v} \cdot \boldsymbol{\Omega}_\lambda) (\mathbf{B}_{0,\lambda} \cdot \mathbf{k}) \right] f_\lambda^{(1)} - \frac{e}{c} (\mathbf{v} \times \mathbf{B}_{0,\lambda}) \cdot \partial_{\mathbf{p}} f_\lambda^{(1)} = e \left[(\tilde{\mathbf{E}} \cdot \mathbf{v}) + \frac{e}{c} (\mathbf{v} \cdot \boldsymbol{\Omega}_\lambda) (\tilde{\mathbf{E}} \cdot \mathbf{B}_{0,\lambda}) \right] \frac{\partial f_\lambda^{(\text{eq})}}{\partial \epsilon_{\mathbf{p}}}, \quad (6)$$

where $\boldsymbol{\Omega}_\lambda = \lambda \hbar \mathbf{p} / (2p^3)$ is the Berry curvature [41], $p \equiv |\mathbf{p}|$, and \mathbf{v} denotes the quasiparticle velocity, defined in Eq. (A4). In the kinetic equation, we also used the following shorthand notations:

$$\kappa_\lambda \equiv \frac{e}{c} (\boldsymbol{\Omega}_\lambda \cdot \mathbf{B}_{0,\lambda}) = \lambda \hbar \frac{e (\hat{\mathbf{p}} \cdot \mathbf{B}_{0,\lambda})}{2cp^2}, \quad (7)$$

$$\tilde{\mathbf{E}} = \mathbf{E} + i \frac{\lambda v_F \hbar}{2\omega p} \mathbf{k} (\hat{\mathbf{p}} \cdot [\mathbf{k} \times \mathbf{E}]), \quad (8)$$

and $\hat{\mathbf{p}} = \mathbf{p}/p$. Note that the second term in Eq. (8) originates from the dependence of the quasiparticle dispersion relation (A3) on the oscillating part of the magnetic field \mathbf{B}' , i.e.,

$$\epsilon_{\mathbf{p}} = v_F p \left[1 - \frac{e}{c} ((\mathbf{B}_{0,\lambda} + \mathbf{B}') \cdot \boldsymbol{\Omega}_\lambda) \right]. \quad (9)$$

By making use of the cylindrical coordinates with the z -axis pointing along the magnetic field $\mathbf{B}_{0,\lambda}$ and ϕ being the azimuthal angle of momentum \mathbf{p} , Eq. (6) can be rewritten in the following form:

$$\frac{v_F e B_{0,\lambda}}{cp} \frac{\partial f_\lambda^{(1)}}{\partial \phi} + i [(1 - \kappa_\lambda) \omega - v_F (\hat{\mathbf{p}} \cdot \mathbf{k})] f_\lambda^{(1)} = e v_F (\hat{\mathbf{p}} \cdot \tilde{\mathbf{E}}) \frac{\partial f_\lambda^{(\text{eq})}}{\partial \epsilon_{\mathbf{p}}}, \quad (10)$$

where we dropped all terms quadratic in $B_{0,\lambda}$. Here it is appropriate to remind that, by construction, the chiral kinetic theory is reliable only to the linear order in $B_{0,\lambda}$ [32, 33].

As one can see, Eq. (10) takes the following conventional form (see, e.g., Ref. [2]):

$$\frac{\partial f_\lambda^{(1)}}{\partial \phi} + i(a_1 + a_2 \cos \phi) f_\lambda^{(1)} = Q(\phi), \quad (11)$$

where the function of the azimuthal angle on the right-hand side is given by

$$Q(\phi) = a_3 \cos(\phi_E - \phi) + a_4 + a_5 \frac{p_{\parallel} k_{\parallel} + p_{\perp} k_{\perp} \cos \phi}{p^2} [E_{\perp} p_{\perp} k_{\parallel} \sin(\phi - \phi_E) + E_{\perp} p_{\parallel} k_{\perp} \sin(\phi_E) - E_{\parallel} k_{\perp} p_{\perp} \sin(\phi)], \quad (12)$$

and

$$a_1 = \frac{cp\omega(1 - \kappa_\lambda)}{ev_F B_{0,\lambda}} - \frac{cp_{\parallel} k_{\parallel}}{eB_{0,\lambda}}, \quad a_2 = -\frac{cp_{\perp} k_{\perp}}{eB_{0,\lambda}}, \quad a_3 = \frac{cp_{\perp} E_{\perp}}{B_{0,\lambda}} \frac{\partial f_\lambda^{(\text{eq})}}{\partial \epsilon_{\mathbf{p}}}, \quad a_4 = \frac{cp_{\parallel} E_{\parallel}}{B_{0,\lambda}} \frac{\partial f_\lambda^{(\text{eq})}}{\partial \epsilon_{\mathbf{p}}}, \quad a_5 = \frac{i\lambda \hbar v_F}{2\omega B_{0,\lambda}} \frac{\partial f_\lambda^{(\text{eq})}}{\partial \epsilon_{\mathbf{p}}}. \quad (13)$$

Here subscripts \parallel and \perp denote parallel and perpendicular components of a vector with respect to the magnetic field direction and ϕ_E denotes the azimuthal angle of \mathbf{E} , which, similarly to ϕ , is measured from the \mathbf{k}_{\perp} direction in the plane perpendicular to the magnetic field.

To the linear order in magnetic field $B_{0,\lambda}$, the equilibrium distribution function (A5) can be expanded as follows:

$$f_\lambda^{(\text{eq})} \approx f_\lambda^{(0)} - \frac{\lambda e v_F \hbar B_{0,\lambda} p_{\parallel}}{2p^2 c} \frac{\partial f_\lambda^{(0)}}{\partial \epsilon} + O(B_{0,\lambda}^2), \quad (14)$$

where $f_\lambda^{(0)}$ is the equilibrium function $f_\lambda^{(\text{eq})}$ at $\mathbf{B}_{0,\lambda} = 0$.

As stated in the Introduction, the main goal of this study is to investigate the spectrum of (pseudo-)magnetic helicons in Weyl materials. The corresponding collective excitations are gapless modes closely related to the cyclotron resonances. By following the same approach that is used in non-relativistic plasmas [2], it is convenient to replace the distribution function $f_\lambda^{(1)}(\phi)$ with a new function,

$$g(\phi) = e^{ia_2 \sin \phi} f_\lambda^{(1)}(\phi), \quad (15)$$

which, in view of Eq. (11), satisfies the following equation:

$$\frac{\partial g}{\partial \phi} + ia_1 g = e^{ia_2 \sin \phi} Q(\phi). \quad (16)$$

By taking into account that $g(\phi)$ is a periodic function of the azimuthal angle ϕ , the solution to Eq. (16) can be obtained in the form of a Fourier series,

$$g(\phi) = \sum_{n=-\infty}^{\infty} g_n e^{in\phi}, \quad (17)$$

where coefficients g_n are given by

$$g_n = -\frac{i}{2\pi(a_1 + n)} \int_0^{2\pi} e^{ia_2 \sin \tau - in\tau} Q(\tau) d\tau. \quad (18)$$

Here the integration over the variable τ can be performed analytically. The corresponding explicit expressions for g_n are presented in Appendix B.

For gapless collective excitations such as helicons, it is convenient to consider the long wavelength limit, i.e., $v_F k \ll \Omega_c|_{p=p^*}$, where $p^* \sim \sqrt{\mu_5^2 + \mu^2 + \pi^2 T^2}/v_F$ is a characteristic momentum in a chiral plasma, and

$$\Omega_c \simeq \frac{ev_F B_{0,\lambda}}{cp} + O(B_{0,\lambda}^2) \quad (19)$$

is an analogue of the cyclotron frequency for massless fermions in the (pseudo)magnetic field that depends on momentum p . In the long wavelength limit, the analysis significantly simplifies because one can neglect the dependence of $f_\lambda^{(1)}$ on the wave vector \mathbf{k} . Furthermore, by utilizing the same approximation as in Ref. [30], we will include only the lowest three (i.e., $n = 0, \pm 1$) Fourier harmonics in the solution. By using the definitions in Eq. (13) and the explicit expressions for the coefficients g_n in Appendix B, we obtain the following results:

$$f_{\lambda,0}^{(1)} = -i \frac{ev_F p_{\parallel} (1 + \kappa_\lambda)}{p\omega} (\mathbf{E} \cdot \hat{\mathbf{z}}) \frac{\partial f_\lambda^{(\text{eq})}}{\partial \epsilon_{\mathbf{p}}}, \quad (20)$$

$$f_{\lambda,\pm}^{(1)} = -i \frac{ev_F p_{\perp} (1 + \kappa_\lambda)}{2p} \frac{E_x \mp iE_y}{\omega \pm \Omega_c} \frac{\partial f_\lambda^{(\text{eq})}}{\partial \epsilon_{\mathbf{p}}} e^{\pm i\phi}, \quad (21)$$

for the $n = 0$ and $n = \pm 1$ Fourier harmonics of $f_\lambda^{(1)}$, respectively. By making use of these results, we derive the expression for the polarization vector \mathbf{P} , i.e.,

$$\begin{aligned} \mathbf{P} = & \sum_{\mathbf{p}, \mathbf{a}} \sum_{\lambda=\pm} \frac{ie}{\omega} \int \frac{d^3 p}{(2\pi\hbar)^3} \left\{ e(\tilde{\mathbf{E}} \times \boldsymbol{\Omega}_\lambda) + \frac{e}{\omega} (\mathbf{v} \cdot \boldsymbol{\Omega}_\lambda) (\mathbf{k} \times \mathbf{E}) + \frac{e}{c} (\delta \mathbf{v} \cdot \boldsymbol{\Omega}_\lambda) \mathbf{B}_{0,\lambda} \right\} f_\lambda^{(\text{eq})} \\ & + \sum_{\mathbf{p}, \mathbf{a}} \sum_{\lambda=\pm} \frac{\lambda e^2 \hbar v_F}{2\omega^2} \int \frac{d^3 p}{(2\pi\hbar)^3} \frac{1}{p} [\mathbf{k} \times \boldsymbol{\Omega}_\lambda] (\hat{\mathbf{p}} \cdot [\mathbf{k} \times \mathbf{E}]) f_\lambda^{(\text{eq})} + \sum_{n=-1}^1 \sum_{\mathbf{p}, \mathbf{a}} \sum_{\lambda=\pm} \frac{ie}{\omega} \int \frac{d^3 p}{(2\pi\hbar)^3} \left[\mathbf{v} + \frac{e}{c} (\mathbf{v} \cdot \boldsymbol{\Omega}_\lambda) \mathbf{B}_{0,\lambda} \right] f_{\lambda,n}^{(1)} \\ & - \sum_{n=-1}^1 \sum_{\mathbf{p}, \mathbf{a}} \sum_{\lambda=\pm} \frac{e}{\omega} \int \frac{d^3 p}{(2\pi\hbar)^3} \epsilon_{\mathbf{p}} f_{\lambda,n}^{(1)} (\mathbf{k} \times \boldsymbol{\Omega}_\lambda) - i \frac{e^3}{2\pi^2 \omega c \hbar^2} (\mathbf{b} \times \mathbf{E}) + i \frac{e^3 b_0}{2\pi^2 \omega^2 \hbar^2} (\mathbf{k} \times \mathbf{E}), \end{aligned} \quad (22)$$

where we used the expression for the current consistent with the local charge conservation [26, 27], see Eqs. (A7), (A10), and (A11). Here,

$$\delta \mathbf{v} = \frac{2ev_F}{c} \hat{\mathbf{p}} (\mathbf{B} \cdot \boldsymbol{\Omega}_\lambda) - \frac{ev_F}{c} \mathbf{B} (\hat{\mathbf{p}} \cdot \boldsymbol{\Omega}_\lambda) = \frac{\lambda \hbar ev_F}{2\omega p^2} \left\{ 2\hat{\mathbf{p}} (\hat{\mathbf{p}} \cdot [\mathbf{k} \times \mathbf{E}]) - [\mathbf{k} \times \mathbf{E}] \right\} \quad (23)$$

is the correction to velocity, which follows from the oscillating magnetic field in the dispersion relation (9). The details of calculation of the polarization vector \mathbf{P} in the limit of small frequencies $\omega \ll \Omega_c|_{p=p^*}$ are given in Appendix C. The final result in the leading order in $B_{0,\lambda}$ takes the following form:

$$4\pi\mathbf{P} = A_1(\mathbf{E} \times \hat{\mathbf{z}}) + A_2(\hat{\mathbf{k}} \times \mathbf{E}) + A_3(\mathbf{b} \times \mathbf{E}) + A_4(\mathbf{E} - \hat{\mathbf{z}}(\mathbf{E} \cdot \hat{\mathbf{z}})) + A_5\hat{\mathbf{z}}(\mathbf{E} \cdot \hat{\mathbf{z}}), \quad (24)$$

where

$$A_1 = \sum_{\lambda=\pm} i \frac{ec\mu_\lambda}{3B_{0,\lambda}v_F^3\hbar^3\pi\omega} (\mu_\lambda^2 + \pi^2T^2) \equiv i \frac{\tilde{A}_1}{\omega}, \quad (25)$$

$$A_2 = i \frac{2ke^2(eb_0 + \mu_5)}{\pi\omega^2\hbar^2} \equiv i \frac{k\tilde{A}_2}{\omega^2}, \quad (26)$$

$$A_3 = -i \frac{2e^3}{\pi\omega c\hbar^2} \equiv i \frac{\tilde{A}_3}{\omega}, \quad (27)$$

$$A_4 = \sum_{\lambda=\pm} \frac{c^2}{3\pi\hbar^3v_F^5B_{0,\lambda}^2} \left(\mu_\lambda^4 + 2\pi^2\mu_\lambda^2T^2 + \frac{7\pi^4T^4}{15} \right), \quad (28)$$

$$A_5 = - \sum_{\lambda=\pm} \frac{2e^2}{3\pi\hbar^3v_F\omega^2} \left(\mu_\lambda^2 + \frac{\pi^2T^2}{3} \right) \equiv \frac{\tilde{A}_5}{\omega^2}. \quad (29)$$

At zero temperature, we obtain

$$\tilde{A}_1 \xrightarrow{T \rightarrow 0} \sum_{\lambda=\pm} \frac{ec\mu_\lambda^3}{3\pi\hbar^3B_{0,\lambda}v_F^3}, \quad (30)$$

$$\tilde{A}_4 \xrightarrow{T \rightarrow 0} \sum_{\lambda=\pm} \frac{c^2\mu_\lambda^4}{3\pi\hbar^3B_{0,\lambda}^2v_F^5}, \quad (31)$$

$$\tilde{A}_5 \xrightarrow{T \rightarrow 0} - \sum_{\lambda=\pm} \frac{2e^2\mu_\lambda^2}{3\pi\hbar^3v_F}. \quad (32)$$

(Note that the other two coefficients, i.e., \tilde{A}_2 and \tilde{A}_3 , do not depend on temperature.) Thus, the dielectric tensor reads

$$\varepsilon^{ml} = \delta^{ml}n_0^2 + 4\pi\chi^{ml} = \delta^{ml}n_0^2 + A_1\epsilon^{ml3} + A_2\epsilon^{mjl}\hat{\mathbf{k}}^j + A_3\epsilon^{mjl}\mathbf{b}^j + A_4(\delta^{ml} - \delta^{m3}\delta^{l3}) + A_5\delta^{m3}\delta^{l3}. \quad (33)$$

It is worth noting that contrary to the case of usual helicons in metals, the dielectric tensor in Weyl materials is modified by the chiral shift \mathbf{b} , see the fourth term in Eq. (33). The dielectric tensor is also affected by the pseudomagnetic field $\mathbf{B}_{0,5}$ and the chiral chemical potential μ_5 . By taking into account that $b_0 = -\mu_5/e$ in equilibrium, we find that ε^{ml} is symmetric with respect to the replacement $(\mathbf{B}_{0,5}, \mu_5) \rightarrow (\mathbf{B}_0, \mu)$.

It is well known that helicons are absent at $\mathbf{k} \perp \mathbf{B}_0$ [1–4]. Therefore, for simplicity, we can set $\mathbf{k} = (0, 0, k_\parallel)$. Then, the characteristic equation (4) takes the form

$$A_3^2\omega^4b_\perp^2 (c^2k^2 - (n_0^2 + A_4)\omega^2) - (n_0^2 + A_5) \left[(c^2k^2 - (n_0^2 + A_4)\omega^2)^2 + \omega^4 (A_1 - A_2 - b_\parallel A_3)^2 \right] = 0. \quad (34)$$

Before solving this equation, let us briefly discuss the role of coefficients A_i (where $i = \overline{1,5}$). As in the case of usual helicons in metals, the existence of pseudomagnetic ones relies on the off-diagonal components of the dielectric tensor, which are given by coefficients A_1 , A_2 , and, in the case of $\mathbf{b} \neq 0$, by A_3 . The first coefficient is related to the nondissipative Hall conductivity, albeit generalized to the case of a pseudomagnetic field and a chiral chemical potential. The coefficient A_2 is proportional to the combination of the energy separation of the Weyl nodes and the chiral chemical potential, $eb_0 + \mu_5$, that vanishes in equilibrium [34, 35]. While in our analysis below we will eventually assume the state of equilibrium, it is interesting to note that the helicon properties could be substantially modified in Weyl materials out of equilibrium, e.g., in steady states with $\mathbf{E}_0 \cdot \mathbf{B}_0 \neq 0$, which are characterized by $eb_0 + \mu_5 \neq 0$. The third term, A_3 , is related to the anomalous Hall effect in Weyl materials [36, 37]. The other two coefficients, i.e., A_4 and A_5 , affect only diagonal components of the dielectric tensor ε^{ml} and, thus, are not crucial for the existence of helicons. However, they could provide quantitative corrections to the dispersion relations of collective excitations.

III. LOW-ENERGY COLLECTIVE MODES

In this section we study the helicon-type solutions to the characteristic equation (34) and analyze their properties. The analysis of the corresponding equation shows that due to the large factor $(n_0^2 + A_5)$, the effect of the chiral shift perpendicular to a background (pseudo-)magnetic field \mathbf{b}_\perp is numerically small for the helicon dispersion relation. Therefore, below we consider only the case $\mathbf{b} = (0, 0, b_\parallel)$, which admits simple analytical solutions for the collective excitation frequencies. Then Eq. (34) reduces to the following equation:

$$(n_0^2\omega^2 - c^2k^2 + \omega^2A_4)^2 + \omega^4(A_1 - A_2 - A_3b_\parallel)^2 = 0, \quad (35)$$

where we also dropped the overall factor $(n_0^2 + A_5)$ because the equation $(n_0^2 + A_5) = 0$ has only a high-energy gapped solution with frequency proportional to the Langmuir (plasma) frequency

$$\Omega_e \equiv \sqrt{\frac{4\alpha}{3\pi\hbar^2} \left(\mu^2 + \mu_5^2 + \frac{\pi^2 T^2}{3} \right)}. \quad (36)$$

Here $\alpha \equiv e^2/(\hbar v_F)$ is the fine structure constant. In view of our approximation of small ω , this solution is unreliable. The corresponding gapped excitations (namely, the chiral magnetic plasmons) were properly analyzed in Refs. [26, 27].

The solutions to Eq. (35) are

$$\omega_\pm = \frac{\pm|\tilde{A}_1 - \tilde{A}_3b_\parallel| + \sqrt{4k(c^2k - \tilde{A}_2)(n_0^2 + \tilde{A}_4) + (\tilde{A}_3b_\parallel - \tilde{A}_1)^2}}{2(n_0^2 + \tilde{A}_4)}, \quad (37)$$

where coefficients \tilde{A}_1 , \tilde{A}_2 , \tilde{A}_3 , and \tilde{A}_4 are given by Eqs. (25) through (29). In the long wavelength limit, we find

$$\omega_+ \simeq \frac{|\tilde{A}_1 - \tilde{A}_3b_\parallel|}{n^2 + \tilde{A}_4} - \frac{\tilde{A}_2k}{|\tilde{A}_1 - \tilde{A}_3b_\parallel|} + k^2 \frac{c^2|\tilde{A}_1 - \tilde{A}_3b_\parallel|^2 - \tilde{A}_2^2(n_0^2 + \tilde{A}_4)}{|\tilde{A}_1 - \tilde{A}_3b_\parallel|^3} + O(k^3), \quad (38)$$

$$\omega_- \simeq \frac{\tilde{A}_2k}{|\tilde{A}_1 - \tilde{A}_3b_\parallel|} + k^2 \frac{c^2|\tilde{A}_1 - \tilde{A}_3b_\parallel|^2 - \tilde{A}_2^2(n_0^2 + \tilde{A}_4)}{|\tilde{A}_1 - \tilde{A}_3b_\parallel|^3} + O(k^3). \quad (39)$$

The gapped solution ω_+ is unreliable since it is outside the validity of the low-frequency approximation used in the derivation. The frequency of the gapless mode is physical and corresponds to a helicon, i.e., $\omega_h = \omega_-$. In the limit of zero temperature, $T \rightarrow 0$, the corresponding result reads

$$\begin{aligned} \omega_h \simeq & \frac{3k(eb_0 + \mu_5)ce\hbar v_F^3(B_0^2 - B_{0,5}^2)}{2B_0c^2\mu(\mu^2 + 3\mu_5^2) - 2B_{0,5}c^2\mu_5(\mu_5^2 + 3\mu^2) + 3(B_0^2 - B_{0,5}^2)e^2\hbar v_F^3b_\parallel} \\ & + \frac{3\pi k^2c^3\hbar^3v_F^3(B_0^2 - B_{0,5}^2)}{2e[2B_0c^2\mu(\mu^2 + 3\mu_5^2) - 2B_{0,5}c^2\mu_5(\mu_5^2 + 3\mu^2) + 3(B_0^2 - B_{0,5}^2)e^2\hbar v_F^3b_\parallel]} \\ & - \frac{9k^2(eb_0 + \mu_5)^2ce\hbar^2v_F^4(B_0^2 - B_{0,5}^2)[B_0^2(\mu^4 + 6\mu^2\mu_5^2 + \mu_5^4) + B_{0,5}^2(\mu^4 + 6\mu^2\mu_5^2 + \mu_5^4) - 8B_0B_{0,5}\mu\mu_5(\mu^2 + \mu_5^2)]}{2[B_0\mu(\mu^2 + 3\mu_5^2) - B_{0,5}\mu_5(\mu_5^2 + 3\mu^2)]^2[2B_0c^2\mu(\mu^2 + 3\mu_5^2) - 2B_{0,5}c^2\mu_5(\mu_5^2 + 3\mu^2) + 9(B_0^2 + B_{0,5}^2)e^2\hbar v_F^3b_\parallel]} + O(k^3), \end{aligned} \quad (40)$$

where we kept only the leading and subleading terms in B_0 and $B_{0,5}$ in the numerators and denominators. It is instructive to consider two special cases

$$\begin{aligned} \omega_h \Big|_{B_0 \rightarrow 0, \mu_5 \rightarrow 0} & \simeq \frac{2b_0B_0ce^4v_F^2k}{\pi c^2\hbar^2\mu\Omega_e^2 + 2B_0e^4v_F^2b_\parallel} + \frac{eB_0c^3\hbar^2\pi v_F^2k^2}{\pi\hbar^2c^2\Omega_e^2\mu + 2B_0e^4v_F^2b_\parallel} - \frac{4B_0ce^7v_F^2k^2b_0^2}{\pi\hbar^2\Omega_e^2(\pi c^2\hbar^2\mu\Omega_e^2 + 6B_0e^4v_F^2b_\parallel)} \\ & \stackrel{b_0 \rightarrow 0}{\simeq} \frac{eB_0c^3\hbar^2\pi v_F^2k^2}{\pi\hbar^2c^2\Omega_e^2\mu + 2B_0e^4v_F^2b_\parallel} + O(k^3), \end{aligned} \quad (41)$$

$$\begin{aligned} \omega_h \Big|_{B_0 \rightarrow 0, \mu \rightarrow 0} & \simeq \frac{2(eb_0 + \mu_5)B_{0,5}ce^3v_F^2k}{\pi c^2\hbar^2\mu_5\Omega_e^2 + 2B_{0,5}e^4v_F^2b_\parallel} + \frac{eB_{0,5}c^3\hbar^2\pi v_F^2k^2}{\pi\hbar^2c^2\Omega_e^2\mu_5 + 2B_{0,5}e^4v_F^2b_\parallel} - \frac{4B_{0,5}ce^5v_F^2k^2(eb_0 + \mu_5)^2}{\pi\hbar^2\Omega_e^2(\pi c^2\hbar^2\mu_5\Omega_e^2 + 6B_{0,5}e^4v_F^2b_\parallel)} \\ & \stackrel{b_0 \rightarrow -\mu_5/e}{\simeq} \frac{eB_{0,5}c^3\hbar^2\pi v_F^2k^2}{\pi\hbar^2c^2\Omega_e^2\mu_5 + 2B_{0,5}e^4v_F^2b_\parallel} + O(k^3). \end{aligned} \quad (42)$$

Note that Eq. (41) agrees with the results obtained in Ref. [30]. It should be emphasized, though, that the default choice of parameters in Ref. [30], i.e., $b_0 \neq 0$ and $\mu_5 = 0$, effectively describes an out-of-equilibrium state of a Weyl plasma. In such a regime, the dispersion is linear in the wave vector. On the other hand, we find that the assumption of equilibrium generically implies a quadratic dispersion relation for the helicon, i.e., it is qualitatively the same as in usual metals. This is due to the fact that the linear term in Eq. (40) is proportional to $eb_0 + \mu_5$ and, thus, vanishes in equilibrium. In essence, this is the same argument that explains the absence of the CME current in Weyl materials in equilibrium [35, 38, 39].

One of the key predictions of this paper is the existence of a gapless helicon-type mode in a Weyl matter without a magnetic field. Indeed, as we see from Eq. (42), a gapless mode can be naturally realized in parity-odd Weyl materials under strain. The corresponding materials in equilibrium are characterized by a strain-induced background pseudomagnetic field $\mathbf{B}_{0,5}$ and a nonzero chiral chemical potential μ_5 , which is determined by the energy separation between the Weyl nodes, i.e., $\mu_5 = -eb_0$. It is natural to call the corresponding gapless mode a pseudomagnetic helicon. In the equilibrium state of the Weyl material, such a helicon has a quadratic dispersion relation, see the second line in Eq. (42). On the other hand, out of equilibrium (e.g., in a steady state with $eb_0 + \mu_5 \neq 0$ produced by external fields with $\mathbf{E}_0 \cdot \mathbf{B}_0 \neq 0$), a nontrivial linear dispersion relation could be realized too.

In order to discuss the qualitative properties of the pseudomagnetic helicons, it is convenient to define a characteristic scale for the chiral shift in Weyl materials. To this end, let us introduce the following reference value:

$$eb^* = 0.3 \frac{\pi \hbar v_F}{c_3}, \quad (43)$$

where $c_3 \approx 25.480 \text{ \AA}$ is the lattice spacing and b^* is comparable to the momentum space separation between the Dirac nodes in Cd_3As_2 [11]. In what follows, we will concentrate only on the equilibrium case $\mu_5 = -eb_0$ with nonzero pseudomagnetic field $\mathbf{B}_{0,5}$ and set $\mathbf{B}_0 = 0$. Also, in our numerical calculations below, we will use the value of the Fermi velocity of Cd_3As_2 [11], i.e., $v_F \approx 1.5 \times 10^8 \text{ cm/s}$. It is expected, of course, that the main qualitative conclusions should remain valid for generic Dirac or Weyl materials.

The effect of the chiral shift parameter $b_{||}$ on the gapless mode ω_h is shown in Fig. 2. As one can see, the chiral shift decreases the helicon frequency. Quantitatively, however, the effect is rather weak.

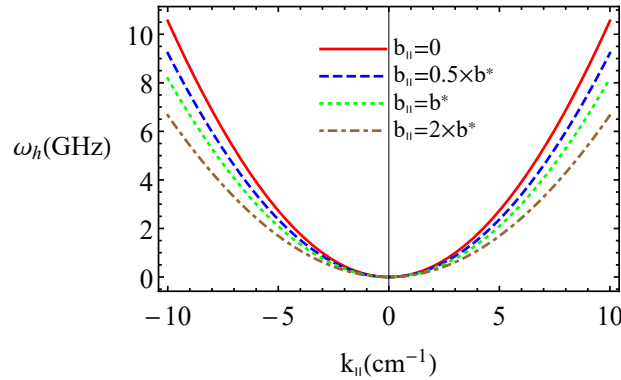


FIG. 2. The helicon dispersion relation $\omega_h = \omega_-$ given by Eq. (37) for $b_{||} = 0$ (red solid line), $b_{||} = 0.5b^*$ (blue dashed line), $b_{||} = b^*$ (green dotted line), and $b_{||} = 2b^*$ (brown dot-dashed line). We set $B_{0,5} = 10^{-2} \text{ T}$, $B_0 = 0$, $\mu_5 = 5 \text{ meV}$, and $\mu = 0$.

The helicon dispersion relations at different values of T , $B_{0,5}$, μ , and μ_5 are plotted in Figs. 3 through 5. Comparing the left and the right panels in Fig. 3 one can see that the dispersion law of the pseudomagnetic helicons changes from the quadratic form at $\mu_5 \neq 0$, $\mu = 0$, and small k to a linear one at $\mu_5 = 0$, $\mu \neq 0$, and large k . In the latter case, the approximate, quadratic in k , expression (39) is valid only for small k . Moreover, the frequency of the helicon mode in the left panel is much lower than in the right one.

Further, we show the dependence of the frequency ω_h on the wave vector k at different values of chiral and electric chemical potentials in the left and right panels in Fig. 4, respectively. In order to be consistent with the approximation of small pseudomagnetic fields

$$\frac{\hbar v_F^2 |eB_{0,5}|}{c(\mu_5^2 + \mu^2 + \pi^2 T^2)} \ll 1, \quad (44)$$

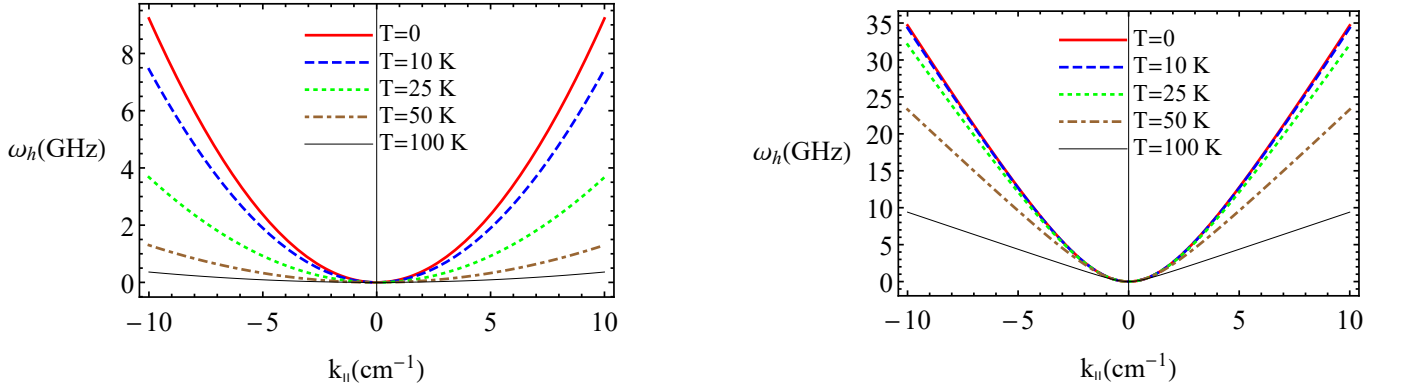


FIG. 3. The frequencies of the collective mode $\omega_h = \omega_-$ defined by Eq. (37). Red solid, blue dashed, green dotted, brown dot-dashed, and black thin solid lines correspond to $T = 0$, $T = 10$ K, $T = 25$ K, $T = 50$ K, and $T = 100$ K, respectively. The left panel is plotted for $\mu_5 = 5$ meV and $\mu = 0$, while the right one represents results obtained for $\mu = 5$ meV and $\mu_5 = 0$. We set $b_{||} = 0.5b^*$, $B_0 = 0$, and $B_{0,5} = 10^{-2}$ T.

we consider only relatively small pseudomagnetic fields $B_{0,5} \lesssim \bar{B}_5$ or sufficiently large electric and chiral chemical potentials $\mu, \mu_5 \gtrsim \bar{\mu}$, where

$$\bar{B}_5 = \frac{c(\mu_5^2 + \mu^2 + \pi^2 T^2)}{e\hbar v_F^2} \xrightarrow{T \rightarrow 0, \mu \rightarrow 0} \frac{c\mu_5^2}{e\hbar v_F^2} \approx 6.853 \times 10^{-4} (\mu_5 [\text{meV}])^2 \text{ T}, \quad (45)$$

$$\bar{\mu} = v_F \sqrt{\frac{\hbar |eB_{0,5}|}{c}} \approx 38.198 \sqrt{B_{0,5} [\text{T}]} \text{ meV}. \quad (46)$$

Similarly to the right panel in Fig. 3, the dispersion law of the pseudomagnetic helicons at $\mu_5 = 0$ and $\mu \neq 0$ (right panel) changes from a quadratic one at small k to a linear one at large k . The dependence of the frequency ω_h on the wave vector k at different values of the pseudomagnetic field is shown in the left and right panels in Fig. 5 for $\mu_5 = 5$ meV, $\mu = 0$ and $\mu_5 = 0$, $\mu = 5$ meV, respectively. Compared to the quadratic decrease of the helicon frequency with μ_5 and μ , the dependency of ω_h on $B_{0,5}$ is almost linear.

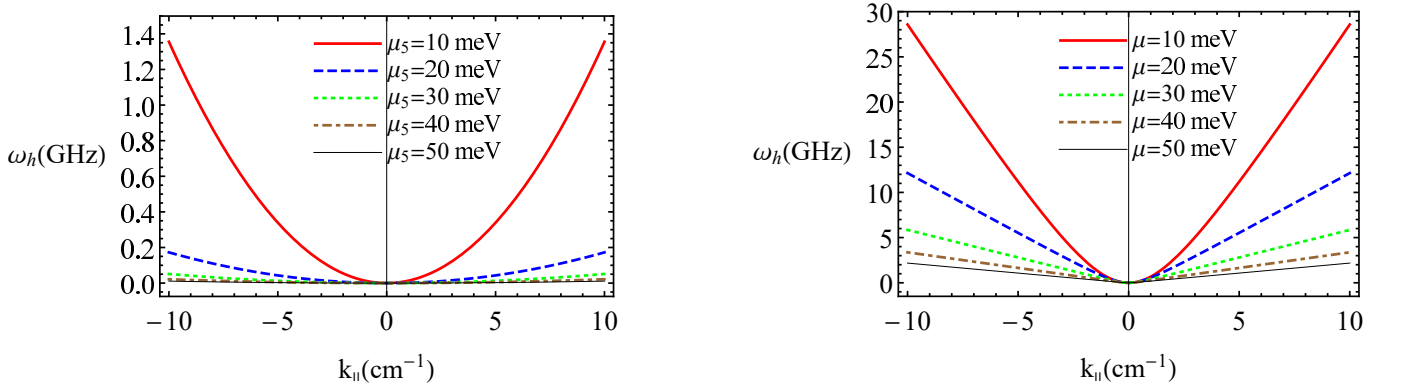


FIG. 4. The dispersion relations of the low-energy collective mode $\omega_h = \omega_-$ defined by Eq. (37). Red solid, blue dashed, green dotted, brown dot-dashed, and black thin solid lines in the left panel correspond to $\mu_5 = 10$ meV, $\mu_5 = 20$ meV, $\mu_5 = 30$ meV, $\mu_5 = 40$ meV, and $\mu_5 = 50$ meV, respectively. The same values, albeit for the electric chemical potential μ , are used in the right panel. The left panel is plotted for $\mu = 0$, while the right one represents results obtained for $\mu_5 = 0$. We set $b_{||} = 0.5b^*$, $T = 0$, $B_0 = 0$, and $B_{0,5} = 10^{-2}$ T.

Finally, we would like to note that the results for a finite background magnetic field \mathbf{B}_0 applied to the system with nonzero chemical potential μ can be obtained by replacing $(\mathbf{B}_{0,5}, \mu_5) \rightarrow (\mathbf{B}_0, \mu)$.

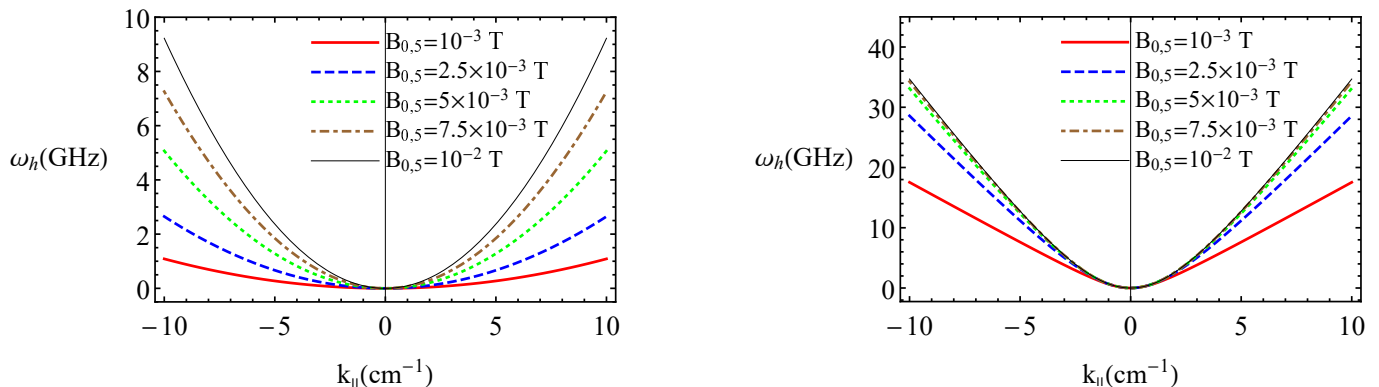


FIG. 5. The dispersion relations of the low-energy collective mode $\omega_h = \omega_-$ defined by Eq. (37). Red solid, blue dashed, green dotted, brown dot-dashed, and black thin solid lines correspond to $B_{0,5} = 10^{-3}$ T, $B_{0,5} = 2.5 \times 10^{-3}$ T, $B_{0,5} = 5 \times 10^{-3}$ T, $B_{0,5} = 7.5 \times 10^{-3}$ T, and $B_{0,5} = 10^{-2}$ T, respectively. The left panel is plotted for $\mu_5 = 5$ meV, $\mu = 0$, while the right one represents results obtained for $\mu_5 = 0$, $\mu = 5$ meV. We set $b_{||} = 0.5b^*$, $T = 0$, and $B_0 = 0$.

IV. SUMMARY

By making use of the consistent chiral kinetic theory, we obtained and analyzed the spectrum of the low-energy gapless helicon-type modes in strained Weyl materials. Unlike the usual helicons, these collective excitations exist even in the absence of a background magnetic field. The necessary ingredients for the existence of these helicons are a strain-induced pseudomagnetic field $\mathbf{B}_{0,5}$ and a chiral chemical potential μ_5 . Note that the latter appears naturally in the equilibrium state of a parity-odd Weyl material with a nonzero energy separation b_0 between the Weyl nodes. We call this new type of collective excitations a *pseudomagnetic helicon*.

We find that in the equilibrium state with $\mu_5 = -eb_0$, when both $\mathbf{B}_{0,5}$ and μ_5 are present, the pseudomagnetic helicon has a conventional, quadratic dependence of its frequency on the wave vector \mathbf{k} . The situation changes qualitatively in the case $B_{0,5} \neq 0$ ($B_0 \neq 0$) but $\mu_5 = 0$ ($\mu = 0$), where the dispersion becomes approximately linear in k . We suggest also that linear dispersion relations for helicons are possible in the out-of-equilibrium states of Weyl materials with $eb_0 + \mu_5 \neq 0$. The corresponding (steady) states of matter could be induced, for example, by applying external electromagnetic fields with $\mathbf{E}_0 \cdot \mathbf{B}_0 \neq 0$. In this paper, we also studied the effects of the temperature, as well as electric and chiral chemical potentials on the properties of helicons. We found, in particular, that all three of them have a tendency to decrease the helicon frequency for a given wave vector.

It is worth noting that the necessary ingredients for the existence of pseudomagnetic helicons are naturally present in Weyl materials, making them ideal platforms to study the anomalous physics. Indeed, the pseudomagnetic field $\mathbf{B}_{0,5}$ can be induced by a strain and the chiral chemical potential μ_5 in equilibrium is determined by the energy separation between Weyl nodes. The effect of the chiral shift \mathbf{b} on the pseudomagnetic helicon is weak, but may be detectable via the change of its frequency.

Last but not least, we would like to propose a simple experimental setup that should allow one to detect pseudomagnetic helicons. Based on the same idea that is used in metals, it requires measuring the amplitude of transmission of an electromagnetic wave through a Weyl crystal as a function of an applied strain (which can be quantified by a bending or torsion angle), or as a function of the frequency at a fixed strain. Because of an interference of standing helicon waves inside the sample, the resulting signal should oscillate as the function of strain, after the strain reaches a sufficiently large magnitude. Note that overcoming a critical value of the strain corresponds to entering the regime of a sufficiently large pseudo-cyclotron frequency compared to the value of the pseudomagnetic helicon frequency. Indeed, this is the condition for the existence of pseudomagnetic helicons that can propagate without suffering too much damping. In such a setup, it is also possible to study the effects of the chiral shift parameter by changing the orientation of the crystal and/or by applying strain along different directions.

ACKNOWLEDGMENTS

The work of E.V.G. was partially supported by the Program of Fundamental Research of the Physics and Astronomy Division of the NAS of Ukraine. The work of V.A.M. and P.O.S. was supported by the Natural Sciences and Engineering Research Council of Canada. The work of I.A.S. was supported by the U.S. National Science Foundation

under Grant No. PHY-1404232.

Appendix A: Equations of the consistent chiral kinetic theory

In this appendix, we briefly review the main aspects of the consistent chiral kinetic theory considered in Refs. [26, 27]. The time evolution of one-particle distribution functions $f_\lambda(t, \mathbf{p}, \mathbf{r})$ for the fermions of chirality $\lambda = \pm$ are governed in the chiral kinetic theory [32, 33] by the following equation in the collisionless limit:

$$\partial_t f_\lambda + \frac{1}{1 + \frac{e}{c}(\mathbf{B}_\lambda \cdot \boldsymbol{\Omega}_\lambda)} \left[\left(e\tilde{\mathbf{E}}_\lambda + \frac{e}{c}(\mathbf{v} \times \mathbf{B}_\lambda) + \frac{e^2}{c}(\tilde{\mathbf{E}}_\lambda \cdot \mathbf{B}_\lambda)\boldsymbol{\Omega}_\lambda \right) \cdot \partial_{\mathbf{p}} f_\lambda + \left(\mathbf{v} + e(\tilde{\mathbf{E}}_\lambda \times \boldsymbol{\Omega}_\lambda) + \frac{e}{c}(\mathbf{v} \cdot \boldsymbol{\Omega}_\lambda)\mathbf{B}_\lambda \right) \cdot \partial_{\mathbf{r}} f_\lambda \right] = 0, \quad (\text{A1})$$

where $\boldsymbol{\Omega}_\lambda = \lambda \hbar \mathbf{p} / (2|\mathbf{p}|^3)$ is the Berry curvature [41], $\tilde{\mathbf{E}}_\lambda = \mathbf{E}_\lambda - (1/e)\partial_{\mathbf{r}}\epsilon_{\mathbf{p}}$, the factor $1/[1 + e(\mathbf{B}_\lambda \cdot \boldsymbol{\Omega}_\lambda)/c]$ accounts for the correct definition of the phase-space volume that satisfies the Liouville's theorem [42, 43], and we introduced the following effective electric and magnetic fields for fermions of a given chirality:

$$\mathbf{E}_\lambda = \mathbf{E} + \lambda \mathbf{E}_5, \quad \mathbf{B}_\lambda = \mathbf{B} + \lambda \mathbf{B}_5. \quad (\text{A2})$$

In Weyl materials, the pseudoelectric field \mathbf{E}_5 can be generated by dynamical deformations of the sample and the pseudomagnetic field \mathbf{B}_5 can be induced by a static torsion or bending [20, 23, 24]. The fermion energy $\epsilon_{\mathbf{p}}$ in the presence of a weak effective magnetic field \mathbf{B}_λ , $\hbar|e\mathbf{B}_\lambda|/(cp^2) \ll 1$, is given by [44]

$$\epsilon_{\mathbf{p}} = v_F p \left[1 - \frac{e}{c}(\mathbf{B}_\lambda \cdot \boldsymbol{\Omega}_\lambda) \right], \quad (\text{A3})$$

where v_F is the Fermi velocity, $p \equiv |\mathbf{p}|$, e is an electric charge ($e < 0$ for the electron), c is the speed of light, and $\hat{\mathbf{p}} = \mathbf{p}/p$. The quasiparticle velocity is defined as follows:

$$\mathbf{v} = \partial_{\mathbf{p}}\epsilon_{\mathbf{p}} = v_F \hat{\mathbf{p}} \left[1 + 2\frac{e}{c}(\mathbf{B}_\lambda \cdot \boldsymbol{\Omega}_\lambda) \right] - \frac{ev_F}{c}\mathbf{B}_\lambda (\hat{\mathbf{p}} \cdot \boldsymbol{\Omega}_\lambda). \quad (\text{A4})$$

In equilibrium, the function f_λ is given by the Fermi-Dirac distribution

$$f_\lambda^{(\text{eq})} = \frac{1}{e^{(\epsilon_{\mathbf{p}} - \mu_\lambda)/T} + 1}, \quad (\text{A5})$$

where $\mu_\lambda = \mu + \lambda\mu_5$ denotes the effective chemical potential for the left- ($\lambda = -$) and right-handed ($\lambda = +$) fermions, μ is the electric chemical potential, μ_5 is the chiral chemical potential, and T is temperature. The equilibrium distribution function for holes (antiparticles) $\bar{f}_\lambda^{(\text{eq})}$ is obtained by replacing $\mu_\lambda \rightarrow -\mu_\lambda$. In addition, in the chiral kinetic equation for the holes distribution function, one should change the sign of the Berry curvature $\boldsymbol{\Omega}_\lambda \rightarrow -\boldsymbol{\Omega}_\lambda$.

By definition, the electric charge density consists of the left- and right-handed fermion contributions, i.e., $\rho = \sum_{\lambda=\pm} \rho_\lambda$, where

$$\rho_\lambda = e \int \frac{d^3p}{(2\pi\hbar)^3} \left[1 + \frac{e}{c}(\mathbf{B}_\lambda \cdot \boldsymbol{\Omega}_\lambda) \right] f_\lambda. \quad (\text{A6})$$

The current densities of the left- and right-handed fermions are [33, 44]

$$\mathbf{j}_\lambda = e \int \frac{d^3p}{(2\pi\hbar)^3} \left[\mathbf{v} + \frac{e}{c}\epsilon_{\mathbf{p}}\mathbf{B}_\lambda(\partial_{\mathbf{p}} \cdot \boldsymbol{\Omega}_\lambda) + \frac{e}{c}(\mathbf{v} \cdot \boldsymbol{\Omega}_\lambda)\mathbf{B}_\lambda + e(\tilde{\mathbf{E}}_\lambda \times \boldsymbol{\Omega}_\lambda) \right] f_\lambda + e\partial_{\mathbf{r}} \times \int \frac{d^3p}{(2\pi\hbar)^3} f_\lambda \epsilon_{\mathbf{p}} \boldsymbol{\Omega}_\lambda. \quad (\text{A7})$$

Therefore, the electric current density is given by $\mathbf{j} = \sum_{\lambda=\pm} \mathbf{j}_\lambda$. Note that the last term in Eq. (A7) is the magnetization current.

By using Eqs. (A6) and (A7) together with the Maxwell equations, one finds that the electric and chiral currents satisfy the following continuity equations:

$$\partial_t \rho_5 + \partial_{\mathbf{r}} \cdot \mathbf{j}_5 = \frac{e^3}{2\pi^2 \hbar^2 c} \left[(\mathbf{E} \cdot \mathbf{B}) + (\mathbf{E}_5 \cdot \mathbf{B}_5) \right], \quad (\text{A8})$$

$$\partial_t \rho + \partial_{\mathbf{r}} \cdot \mathbf{j} = \frac{e^3}{2\pi^2 \hbar^2 c} \left[(\mathbf{E} \cdot \mathbf{B}_5) + (\mathbf{E}_5 \cdot \mathbf{B}) \right]. \quad (\text{A9})$$

The first equation describes the anomalous chiral charge nonconservation [45] and can be understood as a pumping of the chiral charge between the Weyl nodes of opposite chiralities. The second equation, naively, describes the

anomalous local nonconservation of the electric charge when both electromagnetic and pseudoelectromagnetic fields are present. As emphasized in Refs. [26, 27], the conservation of the electric charge in the chiral kinetic theory must be enforced locally by using the consistent definition of the electric current [34, 35, 46]:

$$J^\nu \equiv (c\rho + c\delta\rho, \mathbf{j} + \delta\mathbf{j}), \quad (\text{A10})$$

where

$$\delta j^\mu = \frac{e^3}{4\pi^2\hbar^2 c} \epsilon^{\mu\nu\rho\lambda} A_\nu^5 F_{\rho\lambda} \quad (\text{A11})$$

and $A_\nu^5 = b_\nu + \tilde{A}_\nu^5$ is the axial potential, which is an observable quantity. Indeed, while b_0 and \mathbf{b} correspond to energy and momentum-space separations of the Weyl nodes, respectively, \tilde{A}_ν^5 describes strain-induced axial or, equivalently, pseudoelectromagnetic field directly related to the deformation tensor [19–23]. From a physics viewpoint, the additional contributions to electric current (A11) capture the local changes of ρ and \mathbf{j} associated with the deformations of the crystal lattice that cannot be captured in other ways by the chiral kinetic theory of low-energy quasiparticles.

As is easy to check, the consistent electric current is nonanomalous, $\partial_\nu J^\nu = 0$, and, therefore, the electric charge is locally conserved. It is useful to rewrite the topological contribution (A11) explicitly in components

$$\delta\rho = \frac{e^3}{2\pi^2\hbar^2 c^2} (\mathbf{b} \cdot \mathbf{B}), \quad (\text{A12})$$

$$\delta\mathbf{j} = \frac{e^3}{2\pi^2\hbar^2 c} b_0 \mathbf{B} - \frac{e^3}{2\pi^2\hbar^2 c} (\mathbf{b} \times \mathbf{E}). \quad (\text{A13})$$

where we assumed that the field \mathbf{B}_5 is weak or, in other words, that $\tilde{\mathbf{A}}^5$ is negligible compared to the chiral shift \mathbf{b} .

The first term in $\delta\mathbf{j}$ at $b_0 = -\mu_5/e$ leads to the cancelation of the CME current in the equilibrium state [35] as is required for solids [38, 39]. The second term in Eq. (A13) describes the anomalous Hall effect in Weyl materials [36, 37] in the framework of the semiclassical kinetic theory [26].

Appendix B: Coefficients g_n

In this appendix, we present the explicit results for the Fourier coefficients g_n defined by Eq. (18). The integral representation for the Fourier coefficients is given by

$$\begin{aligned} g_n = & -\frac{i}{2\pi(a_1 + n)} \int_0^{2\pi} d\tau e^{ia_2 \sin \tau - in\tau} \left\{ a_4 - \frac{a_5}{2p^2} E_\perp k_\perp k_\parallel p_\perp^2 \sin \phi_E \right. \\ & + e^{i\phi} \left[\frac{a_3}{2} e^{-i\phi_E} + \frac{a_5}{2p^2} E_\perp k_\perp^2 p_\perp p_\parallel \sin \phi_E + i \frac{a_5}{2p^2} E_\parallel k_\perp k_\parallel p_\perp p_\parallel - i \frac{a_5}{2p^2} E_\perp k_\parallel^2 p_\perp p_\parallel e^{-i\phi_E} \right] \\ & + e^{-i\phi} \left[\frac{a_3}{2} e^{i\phi_E} + \frac{a_5}{2p^2} E_\perp k_\perp^2 p_\perp p_\parallel \sin \phi_E - i \frac{a_5}{2p^2} E_\parallel k_\perp k_\parallel p_\perp p_\parallel + i \frac{a_5}{2p^2} E_\perp k_\parallel^2 p_\perp p_\parallel e^{i\phi_E} \right] \\ & \left. + ie^{2i\phi} \frac{a_5 p_\perp^2}{4p^2} [E_\parallel k_\perp^2 - e^{-i\phi_E} E_\perp k_\perp k_\parallel] - ie^{-2i\phi} \frac{a_5 p_\perp^2}{4p^2} [E_\parallel k_\perp^2 - e^{i\phi_E} E_\perp k_\perp k_\parallel] \right\}, \quad (\text{B1}) \end{aligned}$$

where coefficients a_i , where $i = 1, 5$, are given by Eq. (13). After performing the integration over τ , we derive

$$\begin{aligned} g_n = & -\frac{i}{a_1 + n} \left\{ J_n(a_2) \left[a_4 - \frac{a_5}{2p^2} E_\perp k_\perp k_\parallel p_\perp^2 \sin \phi_E \right] \right. \\ & + J_{n-1}(a_2) \left[\frac{a_3}{2} e^{-i\phi_E} + \frac{a_5}{2p^2} E_\perp k_\perp^2 p_\perp p_\parallel \sin \phi_E + i \frac{a_5}{2p^2} E_\parallel k_\perp k_\parallel p_\perp p_\parallel - i \frac{a_5}{2p^2} E_\perp k_\parallel^2 p_\perp p_\parallel e^{-i\phi_E} \right] \\ & + J_{n+1}(a_2) \left[\frac{a_3}{2} e^{i\phi_E} + \frac{a_5}{2p^2} E_\perp k_\perp^2 p_\perp p_\parallel \sin \phi_E - i \frac{a_5}{2p^2} E_\parallel k_\perp k_\parallel p_\perp p_\parallel + i \frac{a_5}{2p^2} E_\perp k_\parallel^2 p_\perp p_\parallel e^{i\phi_E} \right] \\ & \left. + i J_{n-2}(a_2) \frac{a_5 p_\perp^2}{4p^2} [E_\parallel k_\perp^2 - e^{-i\phi_E} E_\perp k_\perp k_\parallel] - i J_{n+2}(a_2) \frac{a_5 p_\perp^2}{4p^2} [E_\parallel k_\perp^2 - e^{i\phi_E} E_\perp k_\perp k_\parallel] \right\}, \quad (\text{B2}) \end{aligned}$$

where we used the table integral

$$J_n(x) = \frac{1}{2\pi} \int_0^{2\pi} e^{i(n\theta - x \sin \theta)} d\theta, \quad (\text{B3})$$

and the following identities for the Bessel functions: $J_{-n}(x) = (-1)^n J_n(x)$ and $J_n(-x) = (-1)^n J_n(x)$ (see formulas 8.411.1 and 8.404.2 in Ref. [47]).

Appendix C: Polarization vector

In this appendix, we present the details of calculation of the polarization vector \mathbf{P} in the limit of small ω . The polarization vector (22) at $n = 0, \pm 1$ reads as

$$\begin{aligned} \mathbf{P} \simeq & \sum_{\lambda=\pm} \sum_{\mathbf{p}, \mathbf{a}} \frac{ie}{\omega} \int \frac{d^3 p}{(2\pi\hbar)^3} \left[e(\tilde{\mathbf{E}} \times \boldsymbol{\Omega}_\lambda) + \frac{e}{\omega} (\mathbf{v} \cdot \boldsymbol{\Omega}_\lambda) (\mathbf{k} \times \mathbf{E}) + \frac{e}{c} (\delta \mathbf{v} \cdot \boldsymbol{\Omega}_\lambda) \mathbf{B}_{0,\lambda} \right] f_\lambda^{(\text{eq})} \\ & + \sum_{\mathbf{p}, \mathbf{a}} \sum_{\lambda=\pm} \frac{\lambda e^2 \hbar v_F}{2\omega^2} \int \frac{d^3 p}{(2\pi\hbar)^3} \frac{1}{p} f_\lambda^{(\text{eq})} [\mathbf{k} \times \boldsymbol{\Omega}_\lambda] (\hat{\mathbf{p}} \cdot [\mathbf{k} \times \mathbf{E}]) - i \frac{e^3}{2\pi^2 \omega c \hbar^2} (\mathbf{b} \times \mathbf{E}) + i \frac{e^3 b_0}{2\pi^2 \omega^2 \hbar^2} (\mathbf{k} \times \mathbf{E}) \\ & + \sum_{n=-1}^1 \sum_{\lambda=\pm} \sum_{\mathbf{p}, \mathbf{a}} \frac{ie}{\omega} \int \frac{d^3 p}{(2\pi\hbar)^3} v_F \hat{\mathbf{p}} \left[1 + 2 \frac{e}{c} (\mathbf{B}_{0,\lambda} \cdot \boldsymbol{\Omega}_\lambda) \right] g_n e^{in\phi} + O(B_{0,\lambda}^2), \end{aligned} \quad (\text{C1})$$

where we neglected terms of order $O(B_{0,\lambda}^2)$ and terms suppressed by powers of the wave vector, such as $k f_{\lambda,n}^{(1)}$. Also, $\delta \mathbf{v}$ is defined in Eq. (23). Using the expansion of the equilibrium distribution function (14), the first two terms in Eq. (C1) can be represented in the following form:

$$\mathbf{X}_1^{(\text{a})} = \frac{ie^2}{\omega} \int \frac{d^3 p}{(2\pi\hbar)^3} (\mathbf{E} \times \boldsymbol{\Omega}_\lambda) f_\lambda^{(\text{eq})} \simeq -i \frac{e^3 \hbar^2 v_F (\mathbf{E} \times \mathbf{B}_{0,\lambda})}{12c\omega} \int \frac{d^3 p}{(2\pi\hbar)^3} \frac{1}{p^3} \frac{\partial f_\lambda^{(0)}}{\partial \epsilon_{\mathbf{p}}} + O(B_{0,\lambda}^3), \quad (\text{C2})$$

$$\mathbf{X}_1^{(\text{b})} = -\frac{e^2}{\omega} \int \frac{d^3 p}{(2\pi\hbar)^3} \frac{\lambda \hbar v_F}{2\omega p} (\mathbf{E} \cdot [\mathbf{k} \times \hat{\mathbf{p}}]) (\mathbf{k} \times \boldsymbol{\Omega}_\lambda) f_\lambda^{(\text{eq})} \simeq -\frac{v_F e^2}{24\pi^2 \omega^2 \hbar} \int \frac{dp}{p} f_\lambda^{(0)} [\mathbf{k} \times (\mathbf{k} \times \mathbf{E})] + O(B_{0,\lambda}^2), \quad (\text{C3})$$

$$\mathbf{X}_1^{(\text{c})} = \frac{ie^2}{\omega} \int \frac{d^3 p}{(2\pi\hbar)^3} \frac{(\mathbf{v} \cdot \boldsymbol{\Omega}_\lambda)}{\omega} (\mathbf{k} \times \mathbf{E}) f_\lambda^{(\text{eq})} \simeq i (\mathbf{k} \times \mathbf{E}) \frac{\lambda e^2 T}{4\pi^2 \hbar^2 \omega^2} \ln(1 + e^{\mu_\lambda/T}) + O(B_{0,\lambda}^2), \quad (\text{C4})$$

$$\mathbf{X}_1^{(\text{d})} = \frac{ie^2}{\omega} \int \frac{d^3 p}{(2\pi\hbar)^3} \frac{(\delta \mathbf{v} \cdot \boldsymbol{\Omega}_\lambda) \mathbf{B}_{0,\lambda}}{c} f_\lambda^{(\text{eq})} \simeq i \int \frac{d^3 p}{(2\pi\hbar)^3} f_\lambda^{(0)} \frac{e^3 \hbar^2 v_F \mathbf{B}_{0,\lambda}}{4c\omega^2 p^4} (\hat{\mathbf{p}} \cdot [\mathbf{k} \times \mathbf{E}]) = O(B_{0,\lambda}^2), \quad (\text{C5})$$

$$\mathbf{X}_1^{(\text{e})} = -\mathbf{X}_1^{(\text{b})}, \quad (\text{C6})$$

where $f_\lambda^{(0)} = 1/[e^{(\epsilon_{\mathbf{p}}^{(0)} - \mu_\lambda)/T} + 1]$ is the equilibrium function at $\mathbf{B}_{0,\lambda} = 0$ and $\epsilon_{\mathbf{p}}^{(0)} = v_F p$. By adding the contribution of holes (antiparticles), we obtain

$$\begin{aligned} \mathbf{X}_1 = \sum_{\mathbf{p}, \mathbf{a}} (\mathbf{X}_1^{(\text{a})} + \mathbf{X}_1^{(\text{b})} + \mathbf{X}_1^{(\text{c})} + \mathbf{X}_1^{(\text{e})}) &= -i \frac{e^3 \hbar^2 v_F (\mathbf{E} \times \mathbf{B}_{0,\lambda})}{12c\omega} \int \frac{d^3 p}{(2\pi\hbar)^3} \frac{1}{p^3} \left(\frac{\partial f_\lambda^{(0)}}{\partial \epsilon_{\mathbf{p}}} - \frac{\partial \bar{f}_\lambda^{(0)}}{\partial \epsilon_{\mathbf{p}}} \right) \\ &+ \frac{i\lambda T e^2}{4\pi^2 \hbar^2 \omega^2} (\mathbf{k} \times \mathbf{E}) \left[\ln(1 + e^{\mu_\lambda/T}) - \ln(1 + e^{-\mu_\lambda/T}) \right] = i \frac{e^3 v_F (\mathbf{E} \times \mathbf{B}_{0,\lambda})}{24\pi^2 \hbar \omega c T} F\left(\frac{\mu_\lambda}{T}\right) + \frac{i\lambda \mu_\lambda e^2}{4\pi^2 \hbar^2 \omega^2} (\mathbf{k} \times \mathbf{E}) + O(B_{0,\lambda}^2), \end{aligned} \quad (\text{C7})$$

where function

$$F(\nu_\lambda) \equiv -T \int \frac{dp}{p} \left(\frac{\partial f_\lambda^{(0)}}{\partial \epsilon_{\mathbf{p}}} - \frac{\partial \bar{f}_\lambda^{(0)}}{\partial \epsilon_{\mathbf{p}}} \right) \quad (\text{C8})$$

can be easily computed numerically. Thus, Eq. (C1) can be rewritten as

$$\begin{aligned} \mathbf{P} \simeq & \sum_{\lambda=\pm} i \frac{e^3 v_F (\mathbf{E} \times \mathbf{B}_{0,\lambda})}{24\pi^2 \hbar \omega c T} F\left(\frac{\mu_\lambda}{T}\right) - i \frac{e^3}{2\pi^2 \omega c \hbar^2} (\mathbf{b} \times \mathbf{E}) + i \frac{e^2 (eb_0 + \mu_5)}{2\pi^2 \omega^2 \hbar^2} (\mathbf{k} \times \mathbf{E}) \\ & + \sum_{n=\pm} \sum_{\lambda=\pm} \sum_{\mathbf{p}, \mathbf{a}} \frac{\pi e^2 v_F^2}{2\omega} \int_0^\infty \frac{dp}{(2\pi\hbar)^3} \int_{-1}^1 d\cos\theta p_\perp^2 \left(1 + \frac{3\lambda \hbar e p_\parallel B_{0,\lambda}}{2cp^3} \right) \frac{(\mathbf{E} - \hat{\mathbf{z}}(\hat{\mathbf{z}} \cdot \mathbf{E})) - in(\hat{\mathbf{z}} \times \mathbf{E})}{\omega + n\Omega_c} \frac{\partial f_\lambda^{(\text{eq})}}{\partial \epsilon_{\mathbf{p}}} \\ & + \sum_{\lambda=\pm} \sum_{\mathbf{p}, \mathbf{a}} \frac{2\pi e^2 v_F^2}{\omega^2} \int_0^\infty \frac{dp}{(2\pi\hbar)^3} \int_{-1}^1 d\cos\theta \hat{\mathbf{z}}(\mathbf{E} \cdot \hat{\mathbf{z}}) p_\parallel^2 \left(1 + \frac{3\lambda \hbar e p_\parallel B_{0,\lambda}}{2cp^3} \right) \frac{\partial f_\lambda^{(\text{eq})}}{\partial \epsilon_{\mathbf{p}}} + O(B_{0,\lambda}^2). \end{aligned} \quad (\text{C9})$$

Let us consider the case of small frequencies $\omega \ll \Omega_c|_{p=p^*}$, where $p^* \sim \sqrt{\mu_5^2 + \mu^2 + \pi^2 T^2}/v_F$ is a characteristic momentum, relevant for helicons. In the zero order in ω/Ω_c , the fourth term of the above equation equals

$$\begin{aligned} \sum_{n=\pm} \mathbf{P}_n^{(0)} &\simeq \sum_{\lambda=\pm} \sum_{\mathbf{p}, \mathbf{a}} \sum_{n=\pm} [n(\mathbf{E} - \hat{\mathbf{z}}(\hat{\mathbf{z}} \cdot \mathbf{E})) - i(\hat{\mathbf{z}} \times \mathbf{E})] \frac{ev_F c}{12\pi^2 \hbar^3 B_{0,\lambda} \omega} \int_0^\infty dp p^3 \frac{\partial f^{(0)}}{\partial \epsilon_{\mathbf{p}}} + O(B_{0,\lambda}^2) \\ &= \sum_{\lambda=\pm} \sum_{\mathbf{p}, \mathbf{a}} \sum_{n=\pm} [n(\mathbf{E} - \hat{\mathbf{z}}(\hat{\mathbf{z}} \cdot \mathbf{E})) - i(\hat{\mathbf{z}} \times \mathbf{E})] \frac{ecT^3}{2\pi^2 \hbar^3 B_{0,\lambda} v_F^3 \omega} \text{Li}_3(-e^{\mu_\lambda/T}) + O(B_{0,\lambda}^2) \\ &= i \sum_{\lambda=\pm} [\mathbf{E} \times \hat{\mathbf{z}}] \frac{ec\mu_\lambda}{6\pi^2 \hbar^3 B_{0,\lambda} v_F^3 \omega} (\mu_\lambda^2 + \pi^2 T^2) + O(B_{0,\lambda}^2), \end{aligned} \quad (\text{C10})$$

where the replacements $e \rightarrow -e$, $\mu_\lambda \rightarrow -\mu_\lambda$, and $\lambda \rightarrow -\lambda$ in the Berry curvature $\mathbf{\Omega}_\lambda$ was made for holes (antiparticles). To leading order in small ω/Ω_c , we have

$$\begin{aligned} \sum_{n=\pm} \mathbf{P}_n^{(1)} &\simeq - \sum_{\lambda=\pm} \sum_{\mathbf{p}, \mathbf{a}} \sum_{n=\pm} [(\mathbf{E} - \hat{\mathbf{z}}(\hat{\mathbf{z}} \cdot \mathbf{E})) - in(\hat{\mathbf{z}} \times \mathbf{E})] \frac{c^2}{12\pi^2 \hbar^3 B_{0,\lambda}^2} \int_0^\infty dp p^4 \frac{\partial f^{(0)}}{\partial \epsilon_{\mathbf{p}}} + O(B_{0,\lambda}^2) \\ &= - \sum_{\lambda=\pm} \sum_{\mathbf{p}, \mathbf{a}} \sum_{n=\pm} [(\mathbf{E} - \hat{\mathbf{z}}(\hat{\mathbf{z}} \cdot \mathbf{E})) - in(\hat{\mathbf{z}} \times \mathbf{E})] \frac{2c^2 T^4}{\pi^2 \hbar^3 B_{0,\lambda}^2 v_F^5} \text{Li}_4(-e^{\mu_\lambda/T}) + O(B_{0,\lambda}^2) \\ &= \sum_{\lambda=\pm} [\mathbf{E} - \hat{\mathbf{z}}(\mathbf{E} \cdot \hat{\mathbf{z}})] \frac{c^2}{6\pi^2 \hbar^3 B_{0,\lambda}^2 v_F^5} \left(\mu_\lambda^4 + 2\pi^2 \mu_\lambda^2 T^2 + \frac{7\pi^4 T^4}{15} \right) + O(B_{0,\lambda}^2). \end{aligned} \quad (\text{C11})$$

The contribution of g_0 to the polarization vector is given by the last term in Eq. (C1). Its explicit form reads

$$\begin{aligned} \mathbf{P}_0 &\simeq \hat{\mathbf{z}}(\mathbf{E} \cdot \hat{\mathbf{z}}) \sum_{\lambda=\pm} \sum_{\mathbf{p}, \mathbf{a}} \int_0^\infty dp \frac{e^2 v_F^2}{6\pi^2 \hbar^3 \omega^2} p^2 \frac{\partial f_\lambda^{(0)}}{\partial \epsilon_{\mathbf{p}}} + O(B_{0,\lambda}^2) = \hat{\mathbf{z}}(\mathbf{E} \cdot \hat{\mathbf{z}}) \sum_{\lambda=\pm} \sum_{\mathbf{p}, \mathbf{a}} \int_0^\infty dp \frac{e^2 T^2}{3\pi^2 \hbar^3 v_F \omega^2} \text{Li}_2(-e^{\mu_\lambda/T}) \\ &+ O(B_{0,\lambda}^2) = -\hat{\mathbf{z}}(\mathbf{E} \cdot \hat{\mathbf{z}}) \sum_{\lambda=\pm} \frac{e^2}{6\pi^2 \hbar^3 v_F \omega^2} \left(\mu_\lambda^2 + \frac{\pi^2 T^2}{3} \right) + O(B_{0,\lambda}^2). \end{aligned} \quad (\text{C12})$$

In the derivation above, we used the following table integral:

$$\int \frac{d^3 p}{(2\pi)^3} p^{n-2} \frac{\partial f_\lambda^{(0)}}{\partial \epsilon_{\mathbf{p}}} = \frac{T^n \Gamma(n+1)}{2\pi^2 v_F^{n+1}} \text{Li}_n(-e^{\mu_\lambda/T}), \quad n \geq 0, \quad (\text{C13})$$

where $\text{Li}_n(x)$ is the polylogarithm function (see formula 1.1.14 in Ref. [48] where $\text{Li}_n(x) \equiv \text{F}(x, n)$). We also used the following identities for the polylogarithm functions:

$$\text{Li}_2(-e^x) + \text{Li}_2(-e^{-x}) = -\frac{x^2}{2} - \frac{\pi^2}{6}, \quad (\text{C14})$$

$$\text{Li}_3(-e^x) - \text{Li}_3(-e^{-x}) = -\frac{x^3}{6} - \frac{\pi^2 x}{6}, \quad (\text{C15})$$

$$\text{Li}_4(-e^x) + \text{Li}_4(-e^{-x}) = -\frac{x^4}{24} - \frac{\pi^2 x^2}{12} - \frac{7\pi^4}{360}. \quad (\text{C16})$$

-
- [1] N. A. Krall and A. W. Trivelpiece, *Principles of Plasma Physics* (Mc-Graw Hill, New York, 1973).
[2] E. M. Lifshitz and L. P. Pitaevskii, *Physical Kinetics* (Pergamon Press, 1981).
[3] B. W. Maxfield, *Am. J. Phys.* **37**, 241 (1969).
[4] E. A. Kaner and V. G. Skobov, *Sov. Phys. Usp.* **9**, 480 (1967).
[5] J. P. Vallee, *New Astron. Rev.* **55**, 91 (2011).
[6] R. Durrer and A. Neronov, *Astron. Astrophys. Rev.* **21**, 62 (2013).
[7] D. E. Kharzeev, L. D. McLerran, and H. J. Warringa, *Nucl. Phys. A* **803**, 227 (2008).
[8] D. E. Kharzeev, J. Liao, S. A. Voloshin, and G. Wang, *Prog. Part. Nucl. Phys.* **88**, 1 (2016).
[9] C. Kouveliotou, T. Strohmayer, K. Hurley, J. van Paradijs, M. H. Finger, S. Dieters, P. Woods, C. Thompson, and R. S. Duncan, *Astrophys. J.* **510**, L115 (1999).

- [10] S. Borisenko, Q. Gibson, D. Evtushinsky, V. Zabolotnyy, B. Buchner, and R. J. Cava, *Phys. Rev. Lett.* **113**, 027603 (2014).
- [11] M. Neupane, S.-Y. Xu, R. Sankar, N. Alidoust, G. Bian, C. Liu, I. Belopolski, T.-R. Chang, H.-T. Jeng, H. Lin, A. Bansil, F. Chou, and M. Z. Hasan, *Nature Commun.* **5**, 3786 (2014).
- [12] Z. K. Liu, B. Zhou, Y. Zhang, Z. J. Wang, H. M. Weng, D. Prabhakaran, S.-K. Mo, Z. X. Shen, Z. Fang, X. Dai, Z. Hussain, and Y. L. Chen, *Science* **343**, 864 (2014).
- [13] C. Zhang, Z. Yuan, S. Xu, Z. Lin, B. Tong, M. Z. Hasan, J. Wang, C. Zhang, and S. Jia, arXiv:1502.00251.
- [14] S.-Y. Xu, I. Belopolski, N. Alidoust, M. Neupane, G. Bian, C. Zhang, R. Sankar, G. Chang, Z. Yuan, C.-C. Lee, S.-M. Huang, H. Zheng, J. Ma, D. S. Sanchez, B. Wang, A. Bansil, F. Chou, P. P. Shibayev, H. Lin, S. Jia, and M. Z. Hasan, *Science* **349**, 613 (2015).
- [15] B. Q. Lv, H. M. Weng, B. B. Fu, X. P. Wang, H. Miao, J. Ma, P. Richard, X. C. Huang, L. X. Zhao, G. F. Chen, Z. Fang, X. Dai, T. Qian, and H. Ding, *Phys. Rev. X* **5**, 031013 (2015).
- [16] X. Huang, L. Zhao, Y. Long, P. Wang, D. Chen, Z. Yang, H. Liang, M. Xue, H. Weng, Z. Fang, X. Dai, and G. Chen, *Phys. Rev. X* **5**, 031023 (2015).
- [17] I. Belopolski, S.-Y. Xu, Y. Ishida, X. Pan, P. Yu, D. S. Sanchez, M. Neupane, N. Alidoust, G. Chang, T.-R. Chang, Y. Wu, G. Bian, H. Zheng, S.-M. Huang, C.-C. Lee, D. Mou, L. Huang, Y. Song, B. Wang, G. Wang, Y.-W. Yeh, N. Yao, J. Rault, P. Lefevre, F. Bertran, H.-T. Jeng, T. Kondo, A. Kaminski, H. Lin, Z. Liu, F. Song, S. Shin, and M. Z. Hasan, arXiv:1512.09099.
- [18] S. Borisenko, D. Evtushinsky, Q. Gibson, A. Yaresko, T. Kim, M. N. Ali, B. Buechner, M. Hoesch, and R. J. Cava, arXiv:1507.04847.
- [19] M. A. Zubkov, *Annals Phys.* **360**, 655 (2015).
- [20] A. Cortijo, Y. Ferreira, K. Landsteiner, and M. A. H. Vozmediano, *Phys. Rev. Lett.* **115**, 177202 (2015).
- [21] A. Cortijo, D. Kharzeev, K. Landsteiner, and M. A. H. Vozmediano, arXiv:1607.03491.
- [22] A. G. Grushin, J. W. F. Venderbos, A. Vishwanath, and R. Ilan, arXiv:1607.04268.
- [23] D. I. Pikulin, A. Chen, and M. Franz, *Phys. Rev. X* **6**, 041021 (2016).
- [24] T. Liu, D. I. Pikulin, and M. Franz, arXiv:1608.04678.
- [25] H. B. Nielsen and M. Ninomiya, *Nucl. Phys. B* **185**, 20 (1981); **193**, 173 (1981).
- [26] E. V. Gorbar, V. A. Miransky, I. A. Shovkovy, and P. O. Sukhachov, arXiv:1610.07625.
- [27] E. V. Gorbar, V. A. Miransky, I. A. Shovkovy, and P. O. Sukhachov, arXiv:1611.05470.
- [28] O. V. Konstantinov and V. I. Perel, *Sov. Phys. JETP* **11**, 117 (1960).
- [29] P. Aigrain, *Proceedings of the International Conference on Semiconductor Physics* (Czechoslovak Academy of Sciences, Prague, 1961), p. 224.
- [30] F. M. D. Pellegrino, M. I. Katsnelson, and M. Polini, *Phys. Rev. B* **92**, 201407(R) (2015).
- [31] D. T. Son and N. Yamamoto, *Phys. Rev. Lett.* **109**, 181602 (2012).
- [32] M. A. Stephanov and Y. Yin, *Phys. Rev. Lett.* **109**, 162001 (2012).
- [33] D. T. Son and B. Z. Spivak, *Phys. Rev. B* **88**, 104412 (2013).
- [34] K. Landsteiner, *Phys. Rev. B* **89**, 075124 (2014).
- [35] K. Landsteiner, arXiv:1610.04413.
- [36] A. G. Grushin, *Phys. Rev. D* **86**, 045001 (2012).
- [37] P. Goswami and S. Tewari, *Phys. Rev. B* **88**, 245107 (2013).
- [38] M. M. Vazifeh and M. Franz, *Phys. Rev. Lett.* **111**, 027201 (2013).
- [39] G. Basar, D. E. Kharzeev, and H. U. Yee, *Phys. Rev. B* **89**, 035142 (2014).
- [40] W. Freyland, A. Goltzene, P. Grosse, G. Harbeke, H. Lehmann, O. Madelung, W. Richter, C. Schwab, G. Weiser, H. Werheit, and W. Zdanowicz, *Physics of Non-Tetrahedrally Bonded Elements and Binary Compounds I* (Springer-Verlag, Berlin Heidelberg, 1983).
- [41] M. V. Berry, *Proc. R. Soc. A* **392**, 45 (1984).
- [42] D. Xiao, J. Shi, and Q. Niu, *Phys. Rev. Lett.* **95**, 137204 (2005) [*Phys. Rev. Lett.* **95**, 169903 (2005)].
- [43] C. Duval, Z. Horvath, P. A. Horvathy, L. Martina, and P. Stichel, *Mod. Phys. Lett. B* **20**, 373 (2006).
- [44] D. T. Son and N. Yamamoto, *Phys. Rev. D* **87**, 085016 (2013).
- [45] S. L. Adler, *Phys. Rev.* **177**, 2426 (1969); J. S. Bell and R. Jackiw, *Nuovo Cim. A* **60**, 47 (1969).
- [46] W. A. Bardeen, *Phys. Rev.* **184**, 1848 (1969); W. A. Bardeen and B. Zumino, *Nucl. Phys. B* **244**, 421 (1984).
- [47] I. S. Gradshteyn and I. M. Ryzhik, *Table of Integrals, Series and Products* (Academic Press, Orlando, 1980).
- [48] A. Erdelyi, W. Magnus, F. Oberhettinger, and F. G. Tricomi, *Higher Transcendental Functions*, Vol. 1 (Krieger, New York, 1981).